

# A Unified Startup Strategy for Modular Multilevel Converters With Deadbeat Predictive Current Control

Jinyu Wang<sup>ID</sup>, Member, IEEE, Yi Tang<sup>ID</sup>, Senior Member, IEEE, Yang Qi<sup>ID</sup>, Student Member, IEEE, Pengfeng Lin<sup>ID</sup>, Member, IEEE, and Zhenbin Zhang<sup>ID</sup>, Senior Member, IEEE

**Abstract**—Modular multilevel converters (MMCs) are very promising and attractive in medium-/high-voltage applications. One of the main technical challenges associated with MMCs is to precharge all submodule (SM) capacitors to their nominal voltage values during a startup process. This article proposes a simple and effective startup strategy for MMCs based on a deadbeat predictive current control. This strategy can realize a fast precharge for all the SM capacitors from either ac-side or dc-side main voltages without any inrush current and, thus, guarantees a rapid and safe startup of MMCs. With the developed strategy, precharge currents from both ac-side and dc-side can be easily regulated in a closed-loop manner with an excellent dynamic performance. Moreover, conventional controller design and parameter tuning are not necessary, which greatly reduces design burdens and structural complexities of the control algorithm, and consequently facilitates its implementations. Detailed design processes and considerations of the proposed startup strategy are introduced and analyzed. The effectiveness and performance of the developed strategy are verified by sufficient experimental results.

**Index Terms**—Capacitor precharge, deadbeat current control, high-voltage direct current (HVdc) transmission, modular multilevel converter (MMC), startup strategy.

## I. INTRODUCTION

MODULAR multilevel converters (MMCs) have been recognized as the most promising converter topology in medium/high voltage applications and received lots of attention in the past decade. The distinctive advantages of MMCs include

Manuscript received February 10, 2020; revised April 30, 2020 and June 15, 2020; accepted June 24, 2020. Date of publication July 10, 2020; date of current version April 27, 2021. This work was supported by the National Research Foundation, Prime Minister's Office, Singapore under the Energy Innovation Research Programme (EIRP) Energy Storage Grant Call and administrated by the Energy Market Authority under Grant NRF2015EWT-EIRP002 -007. (Corresponding author: Pengfeng Lin.)

Jinyu Wang and Yi Tang are with the School of Electrical and Electronic Engineering, Nanyang Technological University, Singapore 639798 (e-mail: wangjy@ntu.edu.sg; yitang@ntu.edu.sg).

Yang Qi and Pengfeng Lin are with the Interdisciplinary Graduate School, Nanyang Technological University, Singapore 639798 (e-mail: yqj001@e.ntu.edu.sg; linpf001@e.ntu.edu.sg).

Zhenbin Zhang is with the School of Electrical Engineering, Shandong University, Jinan 250061, China (e-mail: zbz@sdu.edu.cn).

Color versions of one or more of the figures in this article are available online at <https://ieeexplore.ieee.org>.

Digital Object Identifier 10.1109/TIE.2020.3007080

flexible scalability, low semiconductor stresses, high efficiency, superior waveform quality, as well as enhanced reliability, etc. These advantages make MMCs very suitable for high-voltage direct current (HVdc) transmission [1], [2]. Besides, MMCs are also considered very attractive in flexible ac transmission systems [3], high-power motor drives [4], static synchronous compensators [5], energy storage systems [6], and power electronic transformers [7].

Despite these distinctive advantages and the wide potential application prospect, MMCs demand a sophisticated control system, in which startup control is one of the major technical challenges [8]–[11]. This is mainly because, different from centralized arranged dc-bus capacitors in conventional voltage source converters, all the submodule (SM) capacitors in MMCs are dispersedly distributed and required to be precharged to their nominal voltage values during a startup process before getting into a normal operation. Otherwise, a large inrush current may be induced at the instant of start, greatly threatening the safe operation of semiconductor devices and capacitors, or even leading to the breakdown of a whole MMC system [9]–[21]. Therefore, a specially designed startup strategy is necessary.

In [9] and [10], MMCs are started with an auxiliary dc power supply installed between the positive and negative dc-buses, whose voltage is equal to one nominal SM capacitor voltage, and then all the SMs are inserted one by one to get charged. This method is straightforward but with a long charging time, as well as high cost and inflexibility. To reduce the charging time, a charging circuit composed of an auxiliary dc power supply and four thyristors for each SM is proposed in [11]. By triggering the thyristors synchronously, all the SM capacitors can be charged together, thus accelerating the startup process. Nevertheless, it has a high control complexity and additional cost to the system. To reduce the cost and improve the flexibility, in [12], an auxiliary dc power supply with a voltage value that can be lower than the nominal SM capacitor voltage is employed, and a special control algorithm is developed to realize normal precharge of the SM capacitors. However, considering the dc-bus voltage is generally very high and, thus, the isolation between the auxiliary dc power supply and the dc-bus becomes a concern. To get rid of the auxiliary dc power supply, in [13], the SM capacitors in the upper arm and lower arm take turns to get charged by the dc-side main voltage with a current-limiting resistor installed in the dc-bus. Similar method is employed

in [14] to charge clamp-double SM (CDSM)-based MMCs by grouping the CDSMs and then charging them group by group. To further reduce the control complexity, in [8], [15], and [16], the precharge of SM capacitors is realized by gradually decreasing the number of inserted SMs. However, all these methods are “open-loop” strategy, which means that the precharge currents during the startup process are uncontrollable. Consequently, they quite rely on the circuit parameters and may lead to overcurrent problems if unexpected disturbances or parameter variations occur. Moreover, the precharge currents decrease or increase exponentially in most of these methods and, thus, result in a long startup process, which is unacceptable in some conditions especially when a quick restart after temporary fault is required [17]–[19].

Different from these “open-loop” control methods, in [18] and [19], a closed-loop control method is proposed. The precharge currents from both the dc side and the ac side can be regulated at a constant value. Therefore, startup speed is significantly improved. Besides, inherited from the robustness of the closed-loop control, this startup method has a good immunity to parameter variations and unexpected disturbances. In [20], the startup of MMCs from ac-side main voltage is controlled in a closed-loop manner by gradually increasing dc-bus voltage to the rated value with a cascaded PI control structure. Another closed-loop startup control method is proposed in [21], in which the resonance between the arm inductor and the SM capacitors is identified as a bandwidth limiting factor of the charging loop. To solve this issue, a capacitor voltage feedforward control is proposed to operate together with an averaging control. However, all the existing closed-loop startup control methods generally design the control loops of the dc-side and ac-side separately with different controllers, which complicates the whole control system. In addition, control parameter tuning of these controllers is a tedious work to ensure system stability under various operating conditions. Moreover, a fast precharge current regulation is hard to achieve with conventional PI controllers in these methods, but it is essential for safety operation and quick startup/restart of an MMC system [18].

This article proposes a novel startup control strategy for MMCs. Compared with the existing both “open-loop” and “closed-loop” control strategies, it has the following features.

- 1) Auxiliary power supplies as well as additional semiconductor devices are not required, and the startup energy directly comes from dc-side or ac-side main voltages.
- 2) This strategy is based on a deadbeat predictive current control and can realize the startup/restart of MMCs with a constant charging current and very fast dynamic response.
- 3) Inherited from the deadbeat predictive current control, conventional controller design and parameter tuning are not necessary.
- 4) This strategy is a unified control algorithm because both the dc-side and the ac-side charging currents can be regulated at the same time. Therefore, separated controllers/control loops design is not necessary.
- 5) Moreover, this startup strategy can be directly employed to realize the normal operating control of MMCs. Therefore, the total design burden/structure complexity of the whole control system can be significantly reduced.

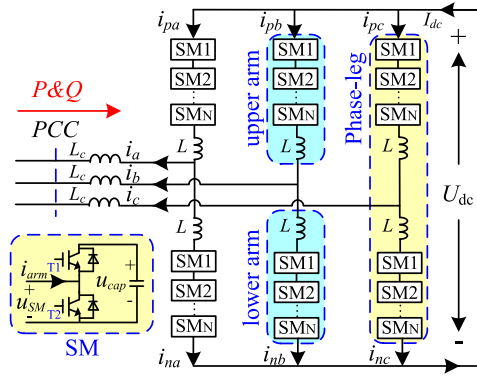


Fig. 1. Circuit configuration of a three-phase MMC.

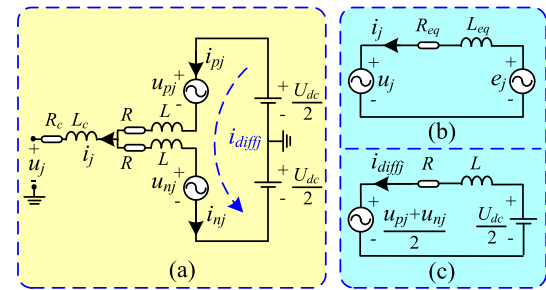


Fig. 2. Equivalent circuit of an MMC. (a) Single-phase equivalent circuit. (b) AC equivalent circuit. (c) DC equivalent circuit.

## II. UNCONTROLLABLE PRECHARGE STAGE OF MMC

### A. Modular Multilevel Converter

The circuit configuration of a typical three-phase MMC with half-bridge SMs is shown in Fig. 1. The SMs in MMC have three states: insert, bypass, and block.

Fig. 2(a) shows the single-phase equivalent circuit of MMC connected to the grid, which can be further divided into the ac and the dc equivalent circuits in Fig. 2(b) and (c), respectively. As shown in Fig. 2,  $L$  and  $R$  are the arm series inductor and arm equivalent resistor, respectively.  $L_c$  and  $R_c$  are the ac-side equivalent inductor and resistor, respectively.  $u_j$  is the ac system voltage at the point of common coupling, and  $i_j$  is the ac-side current ( $j = a, b$ , and  $c$ ).  $u_{pj}$  and  $i_{pj}$  are the upper/lower arm voltage and current, respectively.  $U_{dc}$  is the dc-bus voltage.  $i_{diffj}$  is the inner unbalanced current.  $e_j$  is the electromotive force (EMF) of MMC. Based on the operation principle of MMC and the equivalent circuits in Fig. 2, the following equations can be obtained [22]:

$$L \frac{di_{pj}}{dt} + Ri_{pj} = \frac{U_{dc}}{2} - u_{pj} - L_c \frac{di_j}{dt} - R_c i_j - u_j \quad (1)$$

$$L \frac{di_{nj}}{dt} + Ri_{nj} = \frac{U_{dc}}{2} - u_{nj} + L_c \frac{di_j}{dt} + R_c i_j + u_j \quad (2)$$

$$u_{pj} = \sum_{i=1}^N u_{sm\_pj,i}, \quad u_{nj} = \sum_{i=1}^N u_{sm\_nj,i} \quad (3)$$

$$i_{pj} = i_{diffj} + \frac{i_j}{2}, \quad i_{nj} = i_{diffj} - \frac{i_j}{2} \quad (4)$$

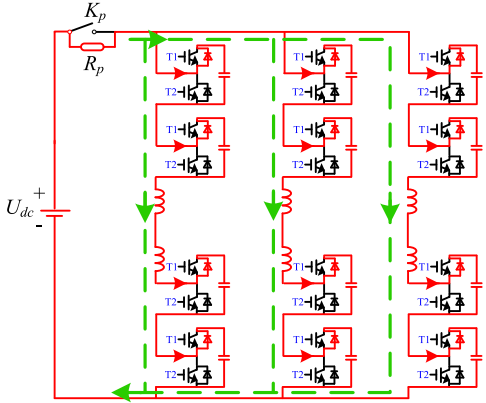


Fig. 3. MMC precharge from dc-side main voltage.

in which  $u_{sm-pj,i}$  and  $u_{sm-nj,i}$  are the  $i$ th SM output voltage of the upper arm and the lower arm in phase  $j$ , respectively. Based on (1)–(4), the ac and the circulating current dynamic equations of MMC can be written as

$$\frac{di_j}{dt} = -\frac{1}{L_{eq}} \left( R_{eq} i_j - \frac{u_{nj} - u_{pj}}{2} + u_j \right) \quad (5)$$

$$\frac{di_{diffj}}{dt} = -\frac{1}{L} \left( Ri_{diffj} + \frac{u_{nj} + u_{pj} - U_{dc}}{2} \right) \quad (6)$$

in which  $L_{eq}$  and  $R_{eq}$  are  $L_{eq} = L_c + L/2$  and  $R_{eq} = R_c + R/2$ , respectively.  $i_{diffj} = I_{dc}/3 + i_{cirj}$ , where  $I_{dc}$  is the dc-bus current and  $i_{cirj}$  is the circulating current. The capacitor voltage dynamic equations of the inserted SMs in MMC can be described by

$$\frac{du_{c-pj,i}}{dt} = -\frac{i_{pj}}{C}, \quad \frac{du_{c-nj,i}}{dt} = -\frac{i_{nj}}{C} \quad (7)$$

where  $u_{c-pj,i}$  and  $u_{c-nj,i}$  are the  $i$ th SM capacitor voltage of the upper arm and the lower arm, respectively. The three main control variables in MMCs are ac, circulating current, and SM capacitor voltages, whose dynamics have been derived in (5)–(7), respectively.

### B. Uncontrollable Precharge Stage of MMC from DC-Side Main Voltage

If MMC is connected to a dc power supply, e.g., its front end is a diode rectifier or is the active dc-bus of HVdc system, the SM capacitors will absorb energy from the dc-side main voltage in an uncontrollable manner.

Fig. 3 shows the MMC precharge circuit from dc-side main voltage where two SMs per arm are taken as an example. A pre-charging (current limiting) resistor is employed to limit the inrush current to avoid breaking devices. This precharge stage is uncontrollable and all the IGBTs are in block state because the voltage of the power supply for the IGBT driving circuit, which generally directly takes power from the local capacitor, is not high enough at the beginning [23], [24]. Therefore, all the SM capacitors will be charged through the freewheeling diode of T1 as shown in Fig. 3. As there are totally  $2N$  SMs per phase in the charging loop, the maximum attainable SM capacitor voltage

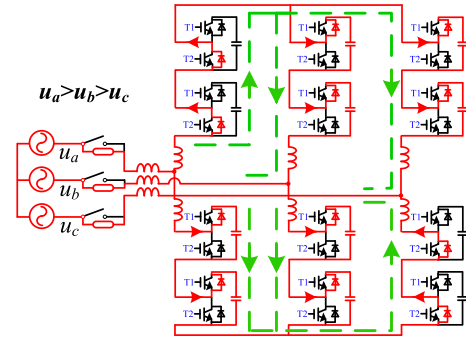


Fig. 4. MMC precharge from ac-side main voltage when  $u_a > u_b > u_c$ .

can be expressed as

$$U_{c\_stage1\_dc} = \frac{U_{dc}}{2N} \quad (8)$$

which is only half of the rated value

$$U_{c\_rated} = \frac{U_{dc}}{N}. \quad (9)$$

As a result, after the uncontrollable precharge stage from the dc-side main voltage, further charging is still necessary to increase the SM capacitor voltage to the rated value.

### C. Uncontrollable Precharge Stage of MMC From AC-Side Main Voltage

If MMC is connected to an ac power supply, e.g., the ac grid, the SM capacitors will absorb energy from the ac-side main voltage in an uncontrollable manner.

Fig. 4 shows the MMC precharge circuit from the ac-side main voltage. Precharging resistors are also employed to limit the inrush current at the start instant. As shown in Fig. 4, at any time, the SM capacitors in the upper arm with the highest phase voltage will be bypassed while the SM capacitors in the other two upper arms will be charged. Oppositely, at any time, the SM capacitors in the lower arm with the lowest phase voltage will be bypassed while the SM capacitors in the other two lower arms will be charged. Consequently, the maximum voltage of total SM capacitors in each arm can be precharged to the amplitude of ac-side line voltage, and thus the SM capacitor voltage can be expressed as

$$U_{c\_stage1\_ac} = \sqrt{3} \frac{U}{N} \quad (10)$$

where  $U$  is the amplitude of the ac-side phase voltage. In normal operation, it is well known that

$$U = NM \frac{U_{c\_rated}}{2} \quad (11)$$

where  $M$  is the modulation index. Substituting (11) into (10) yields

$$U_{c\_stage1\_ac} = \sqrt{3} M \frac{U_{c\_rated}}{2}. \quad (12)$$

Generally,  $M \leq 1$ , and thus, after the uncontrollable precharge stage from the ac-side main voltage, the final SM capacitor

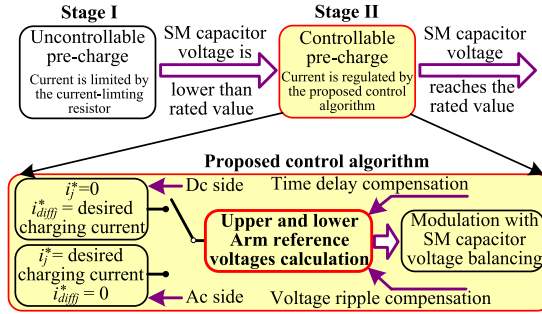


Fig. 5. Overall block diagram of the proposed pre-charging strategy.

voltage is still lower than the rated value and further precharging is still required.

### III. PROPOSED UNIFIED STARTUP STRATEGY FOR MMC

This section proposes a novel unified closed-loop precharge control method based on a deadbeat predictive current control. Deadbeat predictive control is a kind of model-based control method. It provides a very fast dynamic response as conventional MPC, but with a much lower calculation burden because the optimal voltage references are directly calculated without switching state evaluation, cost function calculation, and weighting factor selection [27]. Besides, it usually has a satisfactory steady-state performance because of a modulation stage [28].

Fig. 5 shows the overall block diagram of the proposed precharging strategy. It includes two stages, the uncontrollable stage I introduced above and the controllable stage II which will be introduced as follows. The charging current in stage I is limited by the precharging resistor while it is regulated in stage II by the proposed control algorithm. Therefore, the SM capacitor voltage raises to the rated value with the charging current in stage I and stage II at the desired slew rate. Stage II is introduced in detail as follows.

#### A. Deadbeat Predictive Current Control

The developed deadbeat predictive current control method is based on a discrete model of MMC, which can be derived by discretizing (5)–(7) as follows:

$$i_j(k+1) = i_j(k) - \frac{T_s}{L_{eq}} \times \left[ R_{eq} i_j(k) - \frac{u_{nj}(k) - u_{pj}(k)}{2} + u_j(k) \right] \quad (13)$$

$$i_{diffj}(k+1) = i_{diffj}(k) - \frac{T_s}{L} \times \left[ R i_{diffj}(k) + \frac{u_{nj}(k) + u_{pj}(k) - U_{dc}}{2} \right] \quad (14)$$

$$\begin{cases} u_{c\_pj,i}(k+1) = u_{c\_pj,i}(k) + \frac{i_{pj}(k)}{C} T_s \\ u_{c\_nj,i}(k+1) = u_{c\_nj,i}(k) + \frac{i_{nj}(k)}{C} T_s \end{cases} \quad (15)$$

It is well known that, to realize MMC precharge from dc-side, the circulating current flowing through all the SMs in one phase should be effectively regulated, while to realize MMC precharge

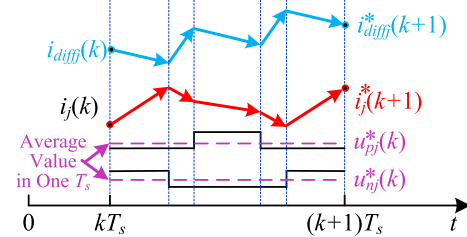


Fig. 6. Principle of the deadbeat predictive current control for MMC in one sampling period.

from ac-side, the ac-side current should be effectively regulated. Therefore, to implement the precharge of MMC from either dc-side or ac-side in one control structure, the control algorithm should have the capability of regulating both circulating current and ac-side current at the same time. This is realized in the proposed method by deriving the optimal arm voltage references.

To obtain the optimal arm voltage references to control the circulating current and the ac-side current, (1) and (2) first should be discretized with forwarding Euler approximation as

$$\begin{cases} L \frac{i_{pj}(k+1) - i_{pj}(k)}{T_s} + R i_{pj}(k) = \frac{U_{dc}}{2} - u_{pj}(k) \\ -L_c \frac{i_j(k+1) - i_j(k)}{T_s} - R_c i_j(k) - u_j(k) \\ L \frac{i_{nj}(k+1) - i_{nj}(k)}{T_s} + R i_{nj}(k) = \frac{U_{dc}}{2} - u_{nj}(k) \\ +L_c \frac{i_j(k+1) - i_j(k)}{T_s} + R_c i_j(k) + u_j(k) \end{cases} \quad (16)$$

Assuming the circulating current and the ac-side current at  $k+1$  time instant can exactly track their respective reference values, and considering (4), (16) can then be rewritten as

$$\begin{cases} L \frac{i_{diffj}^*(k+1) + \frac{i_j(k+1)}{2} - i_{diffj}(k) - \frac{i_j(k)}{2}}{T_s} \\ + R \left[ i_{diffj}(k) + \frac{i_j(k)}{2} \right] \\ = \frac{U_{dc}}{2} - u_{pj}(k) - L_c \frac{i_j(k+1) - i_j(k)}{T_s} - R_c i_j(k) - u_j(k) \\ L \frac{i_{diffj}^*(k+1) - \frac{i_j(k+1)}{2} - i_{diffj}(k) + \frac{i_j(k)}{2}}{T_s} \\ + R \left[ i_{diffj}(k) - \frac{i_j(k)}{2} \right] \\ = \frac{U_{dc}}{2} - u_{nj}(k) + L_c \frac{i_j(k+1) - i_j(k)}{T_s} + R_c i_j(k) + u_j(k) \end{cases} \quad (17)$$

Based on (17), the optimal upper and lower arm voltages that drive the circulating current and the ac-side current to their respective reference values can be derived as

$$\begin{cases} u_{pj}^*(k) = \frac{U_{dc}}{2} - L \frac{i_{diffj}^*(k+1) + \frac{i_j(k+1)}{2} - i_{diffj}(k) - \frac{i_j(k)}{2}}{T_s} \\ - R[i_{diffj}(k)] \\ + \frac{i_j(k)}{2} - L_c \frac{i_j(k+1) - i_j(k)}{T_s} - R_c i_j(k) - u_j(k) \\ u_{nj}^*(k) = \frac{U_{dc}}{2} - L \frac{i_{diffj}^*(k+1) - \frac{i_j(k+1)}{2} - i_{diffj}(k) + \frac{i_j(k)}{2}}{T_s} \\ - R[i_{diffj}(k)] \\ - \frac{i_j(k)}{2} + L_c \frac{i_j(k+1) - i_j(k)}{T_s} + R_c i_j(k) + u_j(k) \end{cases} \quad (18)$$

As depicted in Fig. 6, if the upper and lower arm voltage references  $u_{pj}^*(k)$  and  $u_{nj}^*(k)$  in time period  $k$  (average values represented by purple dashed lines) are modulated (black solid lines) with carriers to control the circulating current and ac-side

current, they can drive them to the given reference values at time instant  $k + 1$  ( $i_j^*(k + 1)$  and  $i_{\text{diff}}^*(k + 1)$ ) with no steady-state errors. Therefore, in the startup process of MMC, the developed deadbeat predictive current control can accurately and effectively regulate both the circulating current and the ac-side current with a very fast dynamic response because of the one control period tracking characteristic. The convergence speed can be deemed as one control period if other influence factors (e.g., overmodulation or measurement errors) are not considered and the system stability is guaranteed. Besides, in this control method, conventional PI or PR controllers and tedious parameter tuning are not required, which greatly reduces the control complexity and calculation burden.

For the deadbeat control in MMC, the inductor variation (parameter mismatch) can affect the control system stability. It has been proved that the stable range is  $0 < L/L_{\text{real}} < 2$ , in which  $L$  is the inductor value used in the algorithm while  $L_{\text{real}}$  is the real inductor value [29], [30]. This condition is generally easy to be met in a reasonably designed circuit with carefully selected devices.

### B. Precharge Control of MMC From the DC-Side

Since the proposed control method can effectively control both the dc-side current and the ac-side current at the same time, the precharge of MMC from the dc-side can be realized by setting the ac-side current reference as zero while dc-side/circulating current reference as a desired value. In this article, constant dc-side charging current/circulating current is adopted to get a fast startup of MMC. The circulating current reference should be smaller than the allowed maximum arm current to ensure a safe operation.

After all the SM capacitors being charged to the nominal voltage value, the circulating current reference should be changed to zero to avoid overcharging, and then MMC can enter standby mode or normal operation mode as required. Because of the excellent dynamic performance of deadbeat predictive control, the state/mode transfer will be very fast and smooth.

### C. Precharge Control of MMC From the AC-Side

After the uncontrollable precharge stage from the ac-side, the maximum SM capacitor voltage is only  $\sqrt{3}/2$  of the rated value. With this voltage, the maximum EMF of MMC can be expressed as

$$E_{\text{stage1\_ac}} = \sqrt{3} \frac{U}{2}. \quad (19)$$

This voltage is smaller than the ac-side voltage  $U$  and thus cannot be directly employed to control the ac-side active power charging current. To solve this problem, the conventional third harmonic injection method is used to increase the dc-bus voltage utilization ratio from  $\sqrt{3}/2$  to 1, and thus, the maximum EMF of MMC can be increased to the same as the ac-side voltage [25].

Fig. 7 shows the power transmission relationship between the ac-side main voltage and MMC, in which Fig. 7(b)–(e) presents the power circle schematics when MMC supplies pure rated active power, supplies pure rated reactive power, absorbs

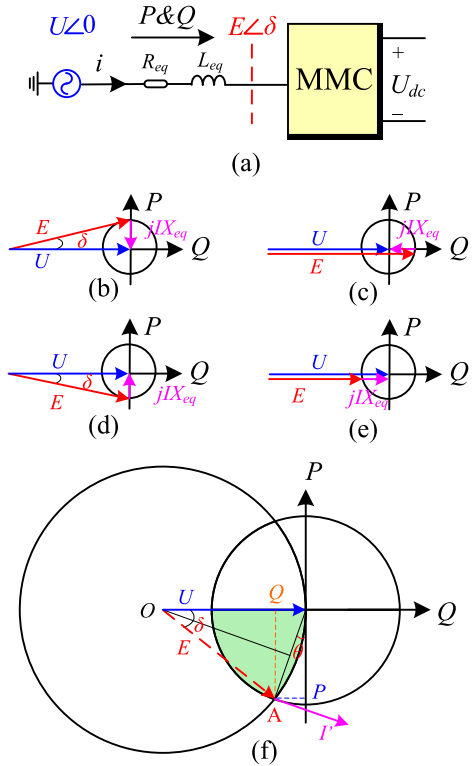


Fig. 7. Power transmission relationship between ac-side grid and MMC.

pure rated active power, and absorbs pure rated reactive power, respectively. To pump the SM capacitor voltage to the rated value after the uncontrollable precharge stage, MMC must absorb some amount of active power from the ac-side main voltage. However, as shown in these subfigures, MMC cannot absorb pure active power because  $E \leq U$ . The green area in Fig. 7(f) presents the MMC power operating range where  $E \leq U$ . Based on the power transmission theory, the transmitted active and reactive powers from the ac-side main voltage to MMC can be expressed as

$$P = -\frac{UE\sin(\delta)}{X_{eq}}; Q = \frac{U^2 - UE\cos(\delta)}{X_{eq}}. \quad (20)$$

Assuming  $E = U$  as shown in Fig. 7(f), the transmitted active and reactive powers at point A can be expressed by

$$P = -\frac{U^2\sin(\delta)}{X_{eq}}; Q = \frac{U^2 - U^2\cos(\delta)}{X_{eq}}. \quad (21)$$

According to the geometrical relationship shown in Fig. 7(f)

$$\sin(\delta) = X_{eq}I' \sqrt{\frac{1}{U^2} - \left(\frac{X_{eq}I'}{2U^2}\right)^2}. \quad (22)$$

Substituting (22) into (21), and considering all the variables are in per-unit value (p.u.)

$$\begin{cases} P = -I' \sqrt{1 - \left(\frac{X_{eq}I'}{2}\right)^2} \\ Q = \frac{1 - \sqrt{1 - (X_{eq}I')^2 + (X_{eq}I')^4/4}}{X_{eq}} \end{cases}. \quad (23)$$

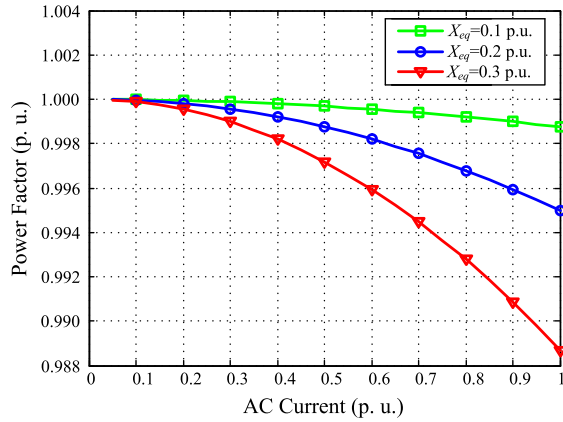


Fig. 8. Power factor of MMC with different ac currents and equivalent inductors.

In general,  $X_{eq}$  in MMC system is designed between 0.1 and 0.3 p.u. Assuming  $X_{eq}$  is respectively equal to 0.1, 0.2, and 0.3 p.u., the power factors (PFs) of the transmitted active and reactive powers ( $PF = P/\sqrt{P^2 + Q^2}$ ) are shown in Fig. 8 with different ac-side current amplitudes. From Fig. 8, along with the increasing of  $X_{eq}$  and the ac-side charging current, the power factor is reducing, which means that to guarantee  $E \leq U$ , the transmitted reactive power should be increased. However, the power factor is still very high. For example, if  $X_{eq} = 0.2$  p.u., the minimum power factor is 0.9987 while it is still as high as 0.9887 even if  $X_{eq} = 0.3$  p.u.

From this analysis, it can be concluded that, by slightly changing power factor, the ac-side charging current can be effectively regulated with the SM capacitor voltage after the uncontrollable precharge stage. The amplitude and phase angle reference of the charging current can be easily obtained from the ac current and power factor shown in Fig. 8.

#### IV. OVERALL STRUCTURE OF THE PROPOSED STARTUP STRATEGY FOR MMC

##### A. Overall Control Structure

The overall control structure of the proposed startup strategy for MMC is shown in Fig. 9, which mainly consists of following:

- 1) an arm voltage calculation module;
- 2) a time delay compensation module;
- 3) an SM capacitor voltage ripple compensation module;
- 4) an SM capacitor voltage balancing control module as well as a phase-shifted carrier (PSC)-based PWM module for modulation of the arm voltage references.

1) The arm voltage calculation module has been introduced in Section III-A. When MMC is started from the dc-side, the ac-side current reference  $i_j^*$  should be set as zero, while the dc-side current reference  $i_{diffj}^*$  should be set as the desired value. When MMC is started from the ac-side, the dc-side current reference  $i_{diffj}^*$  should be set as zero, while the ac-side current reference  $i_j^*$  should be set as the desired value that can be easily obtained based on Fig. 8.

2) It is well known that one sampling period ( $T_s$ ) time delay always exists from a current sampling to a final control signal generation [24]. This time delay can result in inaccurate current tracking and even instability problems. To compensate this time delay, based on (13) and (14), the ac and circulating current at time instant  $k+1$  can be predicted with

$$\begin{cases} \hat{i}_j(k+1) = i_j(k) - \frac{T_s}{L_{eq}} \\ \left[ R_{eq}i_j(k) - \frac{u_{nj}^*(k) - u_{pj}^*(k)}{2} + u_j(k) \right] \\ \hat{i}_{diffj}(k+1) = i_{diffj}(k) - \frac{T_s}{L} \\ \left[ Ri_{diffj}(k) + \frac{u_{nj}^*(k) + u_{pj}^*(k) - U_{dc}}{2} \right] \end{cases}. \quad (24)$$

The optimal arm voltage references at time instant  $k+1$  are

$$\begin{cases} u_{pj}^*(k+1) = \frac{U_{dc}}{2} - L \frac{i_{diffj}^*(k+2) - \frac{\hat{i}_j(k+2)}{2} - \hat{i}_{diffj}(k+1) - \frac{\hat{i}_j(k+1)}{2}}{T_s} \\ - R[\hat{i}_{diffj} \\ (k+1) + \frac{\hat{i}_j(k+1)}{2}] - L_c \frac{i_j^*(k+2) - \hat{i}_j(k+1)}{T_s} - R_c \hat{i}_j(k+1) \\ - \hat{u}_j(k+1) \\ u_{nj}^*(k+1) = \frac{U_{dc}}{2} - L \frac{i_{diffj}^*(k+2) - \frac{\hat{i}_j(k+2)}{2} - \hat{i}_{diffj}(k+1) + \frac{\hat{i}_j(k+1)}{2}}{T_s} \\ - R[\hat{i}_{diffj} \\ (k+1) - \frac{\hat{i}_j(k+1)}{2}] + L_c \frac{i_j^*(k+2) - \hat{i}_j(k+1)}{T_s} + R_c \hat{i}_j(k+1) \\ + \hat{u}_j(k+1) \end{cases}. \quad (25)$$

It can be seen from (25) that the arm voltage references  $u_{pj}^*(k+1)$  and  $u_{nj}^*(k+1)$  can now be obtained at time instant  $k$ , which means they can be obtained one sampling period ahead and consequently the original one sampling period time delay can be compensated.

3) In the charging process of MMC, the SM capacitor voltage is continuously increasing and at the same time even with some low-frequency ripple components if being changed from the ac-side main voltage. If not being properly handled, the time-varying SM capacitor voltage will result in an inaccurate current control and even instability problems of the control system [26]. To solve this issue, the arm voltage references can be first normalized as

$$\begin{cases} u_{p\_n}^*(k) = \frac{u_p^*(k)U_{dc}}{u_{c\_p}(k)} \\ u_{n\_n}^*(k) = \frac{u_n^*(k)U_{dc}}{u_{c\_n}(k)} \end{cases}. \quad (26)$$

before entering the modulation stage. The total capacitor voltage in one arm can be expressed as

$$u_{c\_p}(k) = \sum_{i=1}^N u_{c\_p,i}(k), \quad u_{c\_n}(k) = \sum_{i=1}^N u_{c\_n,i}(k). \quad (27)$$

In this way, the actual arm output voltages  $u_{pj}(k)$  and  $u_{nj}(k)$  will be exactly the same as the references despite the SM capacitor voltage increasing and ripples.

4) In this article, the PSC-PWM and individual SM capacitor voltage balancing control methods are adopted. In Fig. 9,  $s_{pj,i}(k)$  and  $s_{nj,i}(k)$  can be acquired by adding the balancing signals  $\Delta s_{pj,i}$  and  $\Delta s_{nj,i}$  to  $s_{pj}(k)$  and  $s_{nj}(k)$ , respectively,

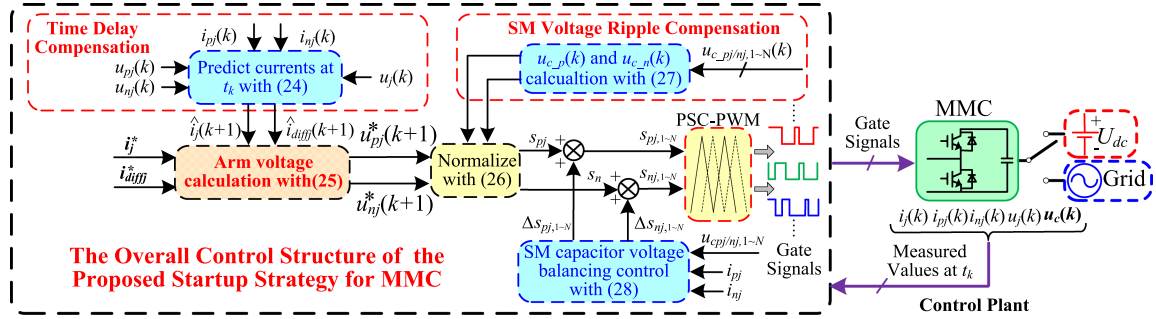


Fig. 9. Overall control structure of the proposed startup strategy for MMC.

which can be expressed as

$$\begin{cases} s_{pj,i}(k) = s_{pj}(k) + k_p i_{pj}(k) \\ \left[ \frac{1}{N} \sum_{i=1}^N u_{c\_pj,i}(k) - u_{c\_pj,i}(k) \right] \\ s_{nj,i}(k) = s_{nj}(k) + k_p i_{nj}(k) \\ \left[ \frac{1}{N} \sum_{i=1}^N u_{c\_nj,i}(k) - u_{c\_nj,i}(k) \right] \end{cases} \quad (28)$$

in which  $k_p$  is a proportional parameter that can affect the balancing speed of the SM capacitor voltages. It can be seen from (28) that, if the  $i$ th SM capacitor voltage is lower than the average value in that arm, the balancing signal together with the arm current [last term in (28)] will inject some amount of active power into this SM capacitor to increase the voltage, while if the  $i$ th SM capacitor voltage is higher than the average value in that arm, the balancing signal together with the arm current will absorb some amount of active power from this SM capacitor to decrease the voltage. Finally, all the SM capacitor voltages in one arm can be balanced to the average value of that arm.

If NLC modulation (more popular when the number of SM is large in high-voltage applications) is required in the control system, this part should be changed from PSC-PWM with individual SM capacitor voltage balancing control to NLC modulation with sorting SM capacitor voltage balancing control while the calculation of reference signals of the upper arm and lower arm (the core of the proposed control algorithm) is the same.

### B. Comparison With Conventional Strategies

To clearly elaborate features of the proposed startup strategy in this article, a detailed comparison of the conventional open-loop strategies [9]–[17], the conventional close-loop strategies [18]–[21], and the proposed strategy is listed in Table I.

In the traditional closed-loop control algorithm, the startup control strategy is independent of the normal operating control strategy, which means that two set control systems (at least four PI controllers) must be designed and operated. Yet, the proposed algorithm can do both start-up control and normal operating control for MMC without any change. Moreover, the proposed algorithm has no PI controllers and, thus, does not need to design the corresponding PI control parameters, which greatly reduces the design burden of the control algorithm.

TABLE I  
COMPARISON OF DIFFERENT STARTUP CONTROL METHODS FOR MMCs

Methods	Open-Loop Methods	Closed-Loop Methods	Proposed Method
<b>Design Burden</b>	Low	High	Low
<b>Structure Complexity</b>	Low	High	Low
<b>Dynamic Performance</b>	Excellent	Moderate	Excellent
<b>Separated Design</b>	Yes	Yes	No
<b>Controllability</b>	Low	High	High
<b>Startup Speed</b>	Slow	Fast	Fast
<b>Robustness</b>	Good	Good	Good

Therefore, the proposed algorithm has a simpler control structure and a much lower design burden compared with the traditional closed-loop control.

The proposed strategy has a very fast dynamic response because of the one control period tracking capability while the traditional closed-loop strategy has a relatively slow dynamic response because of the limited bandwidth.

Both the conventional open-loop and closed-loop control methods generally need to design separated/different controllers or control loops for MMC when it is started from dc-side or ac-side. However, the proposed method can control both the ac-side and dc-side charging currents at the same time and, thus, can be employed for the startup of MMC from either dc-side or ac-side without any change.

With the conventional open-loop control methods, the precharge currents are uncontrollable. Besides, the precharge currents generally decrease or increase exponentially in most of these methods and, thus, result in a long startup process. However, both the conventional closed-loop control methods and the proposed method have higher controllability of the charging currents, and constant charging currents can be maintained in the precharge process. Therefore, they have a faster startup and restart speed compared with the conventional open-loop control methods.

It has been proved that the circuit parameter mismatch degree (the system stable range) can go as high as  $\pm 100\%$  after the

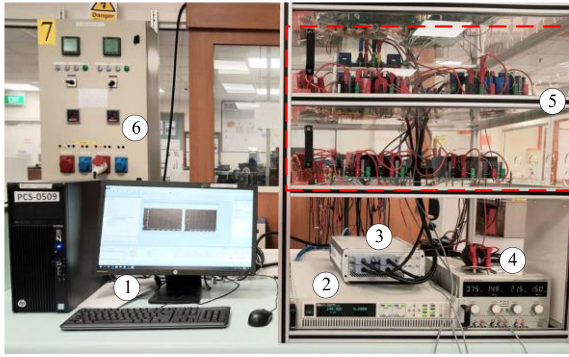


**Fig. 10.** Experimental setup of the three-phase MMC (1) control desk, (2) dc voltage source, (3) DSPACE MicroLabBox, (4) connecting inductor, (5) MMC, (6) and grid.

**TABLE II**  
PARAMETERS OF THE MMC PROTOTYPE

Parameters	Value
AC-side voltage $U$ (phase peak value)	100 V
DC-bus voltage $U_{dc}$	240 V
Connecting inductor $L_c$	2 mH
Connecting resistor $R_c$	0.01 Ω
Load resistor $R_L$ (ac-side)	10 Ω
Load resistor $R_L$ (dc-side)	40 Ω
Number of SMs per arm $N$	3
SM capacitor $C$	0.94 mF
Rated SM capacitor voltage $U_c$	80 V
Arm inductor $L_a$	5 mH
Arm resistor $R_a$	0.01 Ω
Sampling period $T_s$	167 μs
Carrier frequency $f_c$	2 kHz
Rated output frequency $f$	50 Hz

control time delay compensation with deadbeat control [29], [30]. Therefore, the developed control algorithm also has a good robustness as the traditional ones.

## V. EXPERIMENTAL VALIDATION

To verify the validity of the proposed startup control strategy, a three-phase scaled-down MMC prototype shown in Fig. 10 with the circuit parameters listed in Table II has been built. A dSPACE MicroLabBox DS1202 is utilized to implement the developed control algorithm, and a slave Xilinx FPGA inside is utilized to realize the PSC modulation and generate gate signals for all the SMs.

### A. DC-Side Startup Performance

In this startup process, the dc charging current (circulating current) is set as 0.5 A, as shown in Fig. 11. It should be emphasized that the charging current can be set as any value smaller than the maximum allowable arm current. In the experiments, it is set as a small value to see the startup/restart process clearly.

Fig. 11 presents the experiment results of, from top to bottom, the ac-side current, arm currents, circulating current, and SM capacitor voltages. From Fig. 11, after the uncontrollable

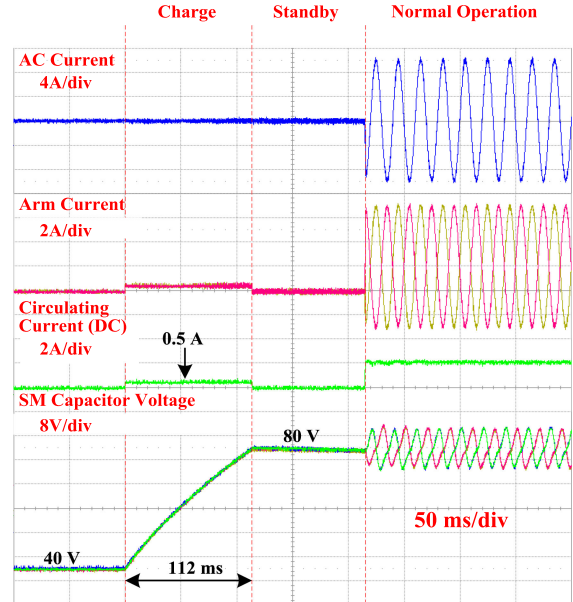


**Fig. 11.** Startup process of MMC from dc-side main voltage with 0.5 A charging current.

precharge stage, all the SM capacitor voltages can be charged to about one half of the rated value 40 V. With the proposed startup control strategy, the charging current can be regulated as a constant value (0.5 A) while the ac-side current can be regulated as zero. All the SM capacitor voltages are increased smoothly to the rated value 80 V. Since the charging current is dc, there is no ripple component in the SM capacitor voltage. After a short charging process (112 ms), the startup of MMC is finished and then MMC can enter standby mode or normal operation mode. In the experiments, MMC enters standby mode first and then normal operation mode. It can be seen from Fig. 11 that the mode switch of MMC is very fast and smooth without any inrush current or overshoot voltage because of the fast-dynamic performance of the developed deadbeat startup control strategy.

### B. AC-Side Startup Performance

In this startup process, the ac charging current (peak value) is set as 1 A. From the experimental results in Fig. 12, after the uncontrollable precharge stage, all the SM capacitor voltages can be charged to about 57.5 V. With the proposed startup control strategy, the ac charging current can be controlled as a constant value (1.0 A) while the dc-side current can be controlled as zero. All the SM capacitor voltages are increased smoothly to the rated value 80 V. Since the charging current is ac, there are some ripple components in the SM capacitor voltage, which is inevitable. After a short charging process (176 ms), the startup of MMC is finished and MMC enters standby mode first and then normal operation mode. From Fig. 12, the mode switch of MMC is very fast and smooth without any inrush current or overshoot voltage because of the fast-dynamic performance of the developed deadbeat startup control strategy.

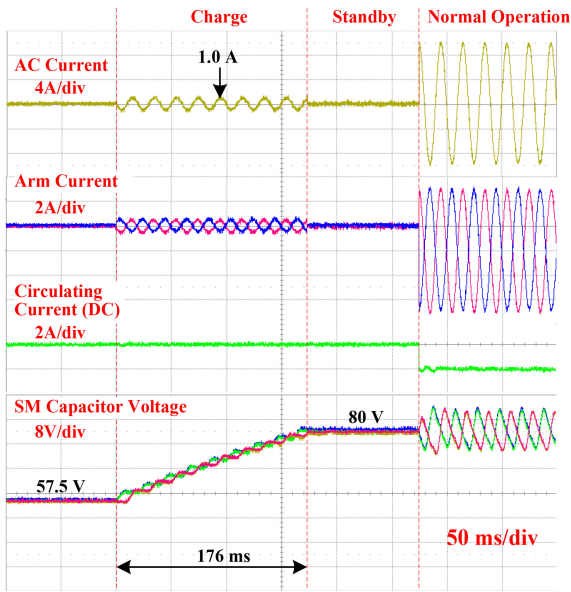


Fig. 12. Startup process of MMC from ac-side main voltage with 1.0 A (peak value) charging current.

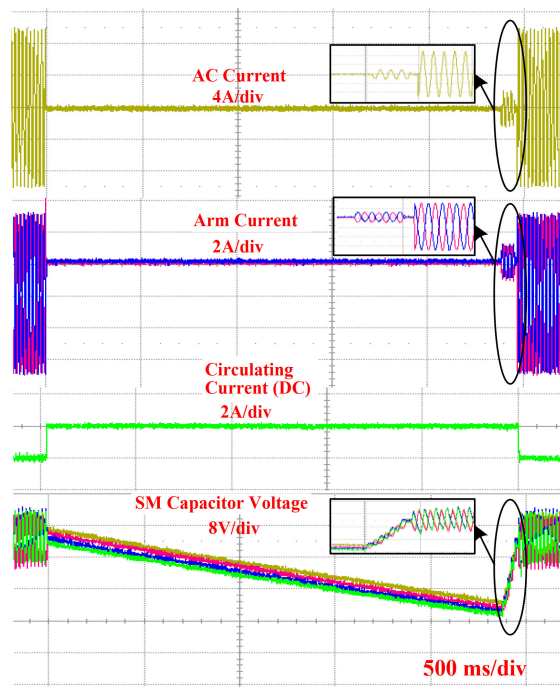


Fig. 14. Restart process of MMC from ac-side main voltage with 2.0-A (peak value) charging current.

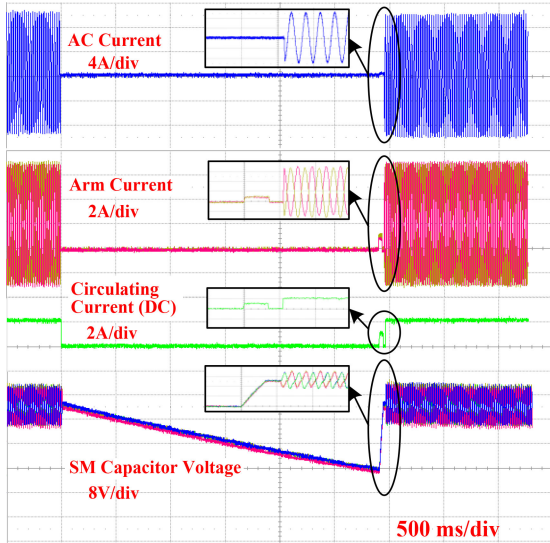


Fig. 13. Restart process of MMC from dc-side main voltage with 1.0-A charging current.

### C. Restart Performance

Restart is a very important feature of MMC especially when fast recovery after temporary fault is required [17]–[19]. In this restart experiment, the MMC is intentionally stopped for a while and then restarted. The corresponding experimental results from the dc-side restart and ac-side restart are, respectively, shown in Figs. 13 and 14. As each SM capacitor is paralleled with a 10-k $\Omega$  bleeding resistor, it can be seen from Figs. 13 and 14 that the capacitor voltages gradually decrease after MMC stops. And once MMC is ordered to restart, all the SM capacitors can be quickly recharged to the rated voltage value from either dc-side main voltage or ac-side main voltage, and thereby, MMC

can immediately resume its normal operation. The whole restart process from both the dc-side and ac-side main voltages as well as the mode switch is very fast and smooth without any inrush current and overshoot voltage. Moreover, the restart speed can be flexibly controlled by simply changing the dc or ac-side charging current reference values.

## VI. CONCLUSION

This article developed a novel unified startup strategy for MMC based on a deadbeat predictive current control. Different from conventional strategies, separated charging controllers/control loops are not required when MMC is started from dc-side and ac-side. Moreover, conventional controller design and parameter tuning are not necessary, which greatly reduces the control complexity and design burden. Inherited from the deadbeat predictive control, the proposed strategy had an excellent current dynamic response, which is very beneficial for the safe operation and smooth state/mode transfer of MMC. The detailed implementation process of this algorithm was presented. The effects of the time-varying SM capacitor voltage during the startup process, as well as the system time delay, were all considered and compensated. The determination of the ac charging current as well as its relationship with the equivalent inductor were quantitatively analyzed. The effectiveness and features of the developed strategy were verified by dc-side startup, ac-side startup as well as dc-side, and ac-side restart experimental results on a three-phase scaled-down MMC prototype.

## REFERENCES

- [1] A. Nami, J. Liang, F. Dijkhuizen, and G. D. Demetriadis, "Modular multilevel converters for HVDC applications: Review on converter cells and functionalities," *IEEE Trans. Power Electron.*, vol. 30, no. 1, pp. 18–36, Jan. 2015.
- [2] G. P. Adam, I. Abdelsalam, J. E. Fletcher, G. Burt, D. Holliday, and S. J. Finney, "New efficient sub-module for modular multilevel converter for multi-terminal HVDC networks," *IEEE Trans. Power Electron.*, vol. 32, no. 6, pp. 4258–4278, Jun. 2017.
- [3] Z. Liu *et al.*, "The start control strategy design of unified power quality conditioner based on modular multilevel converter," in *Proc. IEEE Int. Elect. Mach. Drives Conf.*, May 2013, pp. 933–937.
- [4] S. Du, B. Wu, and N. Zargari, "Delta-channel modular multilevel converter for a variable-speed motor drive application," *IEEE Trans. Ind. Electron.*, vol. 65, no. 8, pp. 6131–6139, Aug. 2018.
- [5] O. J. K. Oghorada, and L. Zhang, "Analysis of star and delta connected modular multilevel cascaded converter-based STATCOM for load unbalanced compensation," *Int. J. Elect. Power Energy Syst.*, vol. 95, pp. 341–352, 2018.
- [6] T. Soong and P. W. Lehn, "Assessment of fault tolerance in modular multilevel converters with integrated energy storage," *IEEE Trans. Power Electron.*, vol. 31, no. 6, pp. 4085–4095, Jun. 2016.
- [7] B. Fan, Y. Li, K. Wang, Z. Zheng, and L. Xu, "Hierarchical system design and control of an MMC-based power-electronic transformer," *IEEE Trans. Ind. Inform.*, vol. 13, no. 1, pp. 238–247, Feb. 2017.
- [8] L. Zhang, J. Qin, X. Wu, S. Debnath, and M. Saeedifard, "A generalized precharge strategy for soft startup process of the modular multilevel converter-based HVDC systems," *IEEE Trans. Ind. Appl.*, vol. 53, no. 6, pp. 5645–5657, Nov./Dec. 2017.
- [9] R. Marquardt and A. Lesnicar, "New concept for high voltage-modular multilevel converter," in *Proc. IEEE Int. Power Electron. Conf.*, 2004, pp. 1–5.
- [10] A. Lesnicar and R. Marquardt, "An innovative modular multilevel converter topology suitable for a wide power range," in *Proc. IEEE Bologna Power Tech Conf.*, 2003, pp. 1–6.
- [11] J. Xu, C. Zhao, B. Zhang, and L. Lu, "New precharge and submodule capacitor voltage balancing topologies of modular multilevel converter for VSC-HVDC application," in *Proc. Asia-Pac. Power Energy Eng. Conf.*, 2011, pp. 1–4.
- [12] K. Tian, B. Wu, S. Du, D. Xu, Z. Cheng, and N. R. Zargari, "A simple and cost-effective precharge method for modular multilevel converters by using a low-voltage DC source," *IEEE Trans. Power Electron.*, vol. 31, no. 7, pp. 5321–5329, Jul. 2016.
- [13] A. Das, H. Nademi, and L. Norum, "A method for charging and discharging capacitors in modular multilevel converter," in *Proc. Conf. IEEE Ind. Electron. Soc.*, 2011, pp. 1058–1062.
- [14] Y. Xue, Z. Xu, and G. Tang, "Self-start control with grouping sequentially precharge for the C-MMC-based HVDC system," *IEEE Trans. Power Del.*, vol. 29, no. 1, pp. 187–198, Feb. 2014.
- [15] K. Shi, F. Shen, D. Lv, P. Lin, M. Chen, and D. Xu, "A novel start-up scheme for modular multilevel converter," in *Proc. IEEE Energy Convers. Congr. Expo.*, pp. 4180–4187, 2012.
- [16] J. Qin, S. Debnath, and M. Saeedifard, "Precharge strategy for soft startup process of modular multilevel converters based on various sm circuits," in *Proc. IEEE Appl. Power Electron. Conf. Expo.*, Mar. 2016, pp. 1528–1533.
- [17] X. Li, Q. Song, W. Liu, H. Rao, S. Xu, and L. Li, "Protection of nonpermanent faults on dc overhead lines in MMC-based HVDC systems," *IEEE Trans. Power Del.*, vol. 28, no. 1, pp. 483–490, Jan. 2013.
- [18] B. Li *et al.*, "Closed-loop precharge control of modular multilevel converters during start-up processes," *IEEE Trans. Power Electron.*, vol. 30, no. 2, pp. 524–531, Feb. 2015.
- [19] B. Li, Y. Zhang, D. Xu, and R. Yang, "Start-up control with constant precharge current for the modular multilevel converter," in *Proc. 2014 IEEE 23rd Int. Symp. Ind. Electron.*, 2014, pp. 673–676.
- [20] Y. Yang, Q. Ge, M. Lei, X. Wang, X. Yang, and R. Gou, "Precharge control strategies of modular multilevel converter," in *Proc. Int. Conf. Elect. Mach. Syst.*, Oct 2013, pp. 1842–1845.
- [21] X. Shi, B. Liu, Z. Wang, Y. Li, L. M. Tolbert, and F. Wang, "Modeling, control design, and analysis of a startup scheme for modular multilevel converters," *IEEE Trans. Ind. Electron.*, vol. 62, no. 11, pp. 7009–7024, Nov. 2015.
- [22] J. Wang and P. Wang, "Power decoupling control for modular multilevel converter," *IEEE Trans. Power Electron.*, vol. 33, no. 11, pp. 9296–9309, Nov. 2018.
- [23] M. Glinka, "Prototype of multiphase modular-multilevel-converter with 2 MW power rating and 17-level-output-voltage," in *Proc. IEEE Power Electron. Spec. Conf.*, Jun. 2004, pp. 2572–2576.
- [24] T. Modeer, S. Norrga, and H.-P. Nee, "High-voltage tapped-inductor buck converter auxiliary power supply for cascaded converter submodules," in *Proc. Conf. IEEE Energy Convers. Congr. Expo.*, 2012, pp. 19–25.
- [25] M. J. Duran, F. Salas, and M. R. Arahal, "Bifurcation analysis of five-phase induction motor drives with third harmonic injection," *IEEE Trans. Ind. Electron.*, vol. 55, no. 5, pp. 2006–2014, May 2008.
- [26] D. Zhou, S. Yang, and Y. Tang, "Model predictive current control of modular multilevel converters with phase-shifted pulse-width modulation," *IEEE Trans. Ind. Electron.*, vol. 66, no. 6, pp. 4368–4378, Jun. 2019.
- [27] P. Cortés, M. P. Kazmierkowski, R. M. Kennel, D. E. Quevedo, and J. Rodríguez, "Predictive control in power electronics and drives," *IEEE Trans. Ind. Electron.*, vol. 55, no. 12, pp. 4312–4324, Dec. 2018.
- [28] C. R. D. Osório, G. S. da Silva, J. C. Giacomini, and C. Rech, "Comparative analysis of predictive current control techniques applied to single-phase grid-connected inverters," in *Proc. Brazilian Power Electron. Conf.*, 2017, pp. 1–6.
- [29] Z. Gong, X. Wu, P. Dai, and R. Zhu, "Modulated model predictive control for MMC-based active front-end rectifiers under unbalanced grid conditions," *IEEE Trans. Ind. Electron.*, vol. 66, no. 3, pp. 2398–2409, Mar. 2019.
- [30] J. Wang, Y. Tang, P. Lin, X. Liu, and J. Pou, "Deadbeat predictive current control for modular multilevel converters with enhanced steady-state performance and stability," *IEEE Trans. Ind. Electron.*, vol. 35, no. 7, pp. 6878–6894, Jul. 2020.



**Jinyu Wang** (Member, IEEE) received the B.Eng. degree in electrical engineering and M.Eng. degree in power electronics from Jilin University, Changchun, China, in 2010 and 2013, respectively, and the Ph.D. degree in power system from Shandong University, Jinan, China, in 2017.

He is currently a Research Fellow with Nanyang Technological University, Singapore. His current research interests include power electronics, multilevel converters, renewable energy generation and integration techniques as well as stability analysis and control of modular multilevel converter based HVdc.



**Yi Tang** (Senior Member, IEEE) received the B.Eng. degree in electrical engineering from Wuhan University, Wuhan, China, in 2007, and the M.Sc. and Ph.D. degrees in power engineering from the School of Electrical and Electronic Engineering, Nanyang Technological University, Singapore, in 2008 and 2011, respectively.

From 2011 to 2013, he was a Senior Application Engineer with Infineon Technologies Asia Pacific, Singapore. From 2013 to 2015, he was a Postdoctoral Research Fellow with Aalborg University, Aalborg, Denmark. Since March 2015, he has been with Nanyang Technological University, Singapore as an Assistant Professor. He is the Cluster Director of the Advanced Power Electronics Research Program with the Energy Research Institute, Nanyang Technological University.

Dr. Tang was the recipient of the Infineon Top Inventor Award in 2012, the Early Career Teaching Excellence Award in 2017, and four IEEE Prize Paper Awards. He serves as an Associate Editor for the IEEE TRANSACTIONS ON POWER ELECTRONICS and the IEEE JOURNAL OF EMERGING AND SELECTED TOPICS IN POWER ELECTRONICS.



**Yang Qi** (Student Member, IEEE) received the B.Sc. degree in electrical engineering from Xi'an Jiaotong University, China, in 2016. He is currently working toward the Ph.D. degree in electrical engineering with Interdisciplinary Graduate School, Nanyang Technological University, Singapore.

He is an exchange student with University of Houston in 2019. His research interests include control and grid integration of energy storage systems, power system modeling, and stability analysis.



**Pengfeng Lin** (Member, IEEE) received the B.S. and M.S. degrees from Southwest Jiaotong University, China, in 2013 and 2015, respectively, and the Ph.D. degree from Nanyang Technological University, Singapore, in 2019, all in electrical engineering.

He is currently working with Energy Research Institute @ NTU (Eri@N), Singapore, as a Research Fellow. His research interests include power system stability/reliability analyses, smart grid cyber-physical security, and artificial intelligence analytic.



**Zhenbin Zhang** (Senior Member, IEEE) was born in Shandong, China, in 1984. He received the B.S. degree in electrical engineering and automation from Harbin Engineering University, Harbin, China, in 2008, the M.S. degree in control theory and engineering from Shandong University, Jinan, China, in 2011, and the Ph.D. degree in energy and electrical engineering from the Institute for Electrical Drive Systems and Power Electronics (EAL), Technical University of Munich (TUM), Munich, Germany, in 2016.

From 2016 to 2017, he was a Research Fellow and the Team Leader with the Modern Control Strategies for Electrical Drives Group, EAL, TUM. Since 2017, he has been a Full Professor of Electrical Engineering with Shandong University, Jinan. Since 2018, he has been a Guest Professor with TUM. In 2019, he was appointed as the National Distinguished Expert (supported by the Youth Talent Program) of China. His research interests include power electronics and electrical drives, sustainable energy systems, and smart grids.

Dr. Zhang was the recipient of the VDE-Award, Germany, in 2017. He is currently an Associate Editor of the IEEE TRANSACTION IN INDUSTRIAL ELECTRONICS.